Polymeric Nanogels with Tailorable Degradation Behavior

Yinan Chen, Mies J. van Steenbergen, Dandan Li, Joep B. van de Dikkenberg, Twan Lammers, Cornelus F. van Nostrum, Josbert M. Metselaar, Wim E. Hennink*

The aim of this study is to design a polymeric nanogel system with tailorable degradation behavior. To this end, hydroxyethyl methacrylate-oligoglycolates-derivatized poly(hydroxypropyl methacrylamide) (pHPMAm-Gly-HEMA) and hydroxyethyl methacrylamide-oligoglycolates-derivatized poly(hydroxyethyl methacrylamide) (pHEMAm-Gly-HEMAm) are synthesized and characterized. pHEMAm-Gly-HEMAm shows faster hydrolysis rates of both carbonate and glycolate esters than the same ester groups of pHPMAm-Gly-HEMA. pHEMAm-Gly-HEMAm nanogels have tailorable degradation kinetics from 24 h to more than 4 d by varying their crosslink densities. It is shown that the release of a loaded macromolecular model drug is controlled by degradation of nanogels. The nanogels show similar cytocompatibility as PLGA nanoparticles and are therefore considered to be attractive systems for drug delivery.

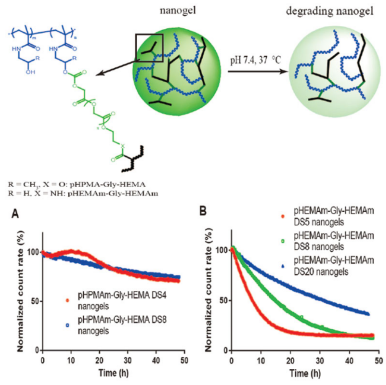

1. Introduction

Nanogels are nanosized hydrogels composed of hydrophilic polymeric networks.[1–4] In addition to hydrogel properties such as high water content, good biocompatibility, and controlled release of payloads,[5,6] the small particle size warrants the use of nanogels as an injectable colloidal drug delivery system for example intravenous therapy.[7–12] Physically self-assembled nanogels that are crosslinked exploiting hydrophobic interactions or/and hydrogen bonding have been developed,[13–16] but nanogels prepared by chemical crosslinking usually have better stability.[17,18] Furthermore, the use of stimulus-sensitive crosslinks enables chemically crosslinked nanogels to respond to a certain external physical or a physiological trigger.[19–21]

Introduction of labile groups in the crosslinks allows the nanogels to degrade and release their payload under physiological conditions.[20] Earlier Ulbrich et al[22,23] prepared macroscopic hydrogels using hydrolyzable —COONHCO— groups as crosslinks, and poly(N-(2-hydroxypropyl) methacrylamide) (pHPMAm) as hydrophilic building blocks. At pH 7.4 and 37 °C, the degradation time of these hydrogels varied from 4 to 76 h. In our department, we developed macroscopic dextran hydrogels crosslinked by polymerization of hydroxyethyl coupled to dextran via a carbonate ester or an oligolactate spacer.[24] Degradation studies showed that the erosion times of

Y. Chen, M. J. van Steenbergen, D. Li, J. B. van de Dikkenberg, Prof. T. Lammers, Dr. C. F. van Nostrum, Prof. W. E. Hennink
Department of Pharmaceutics
Utrecht Institute for Pharmaceutical Sciences
Utrecht University
3584 CG, Utrecht, The Netherlands
E-mail: w.e.hennink@uu.nl
Prof. T. Lammers, Dr. J. M. Metselaar
Department of Targeted Therapeutics
MIRA Institute for Biomedical Engineering and Technical Medicine
University of Twente
7522 NB, Enschede, The Netherlands
Prof. T. Lammers, Dr. J. M. Metselaar
Department of Nanomedicine and Theranostics
Institute for Experimental Molecular Imaging
RWTH Aachen University Clinic
52074 Aachen, Germany

DOI: 10.1002/mabi.201600031

these hydrogels depended on the chemical nature of the crosslinks and the crosslink density, and could be tailored from days to months.[24–26]

The work presented here is centered on pHPMAm and poly (N-(2-hydroxyethyl)methacrylamide) (pHEMAm) nanogels crosslinked using different hydrolytically sensitive groups. We selected pHPMAm and pHEMAm as building blocks of the nanogels because these polymers are water soluble and have shown excellent biosafety in preclinical (both polymers) and clinical (pHPMAm) studies. Additionally, these synthetic polymers can be functionalized either by coupling of for example drugs, imaging agents, and targeting ligands to the hydroxyl functional groups of the polymers or by copolymerization of HEMAm/HPMAm with other (functional) monomers.[27–31] In the literature, it has been reported that polymer-oligoglycolates have better aqueous solubility and faster degradation than polymer-oligolactates.[24,32,33] Therefore, oligoglycolates were chosen as hydrolytically sensitive groups in the crosslinks of the gels. To this end hydroxypropyl methacrylate (HEMA) and HEMAm were esterified with oligoglycolates. Subsequently, HEMA- and HEMAm-oligoglycolates were coupled to pHPMAm and pHEMAm respectively and with different degrees of substitution, and the obtained modified polymers were used as building blocks of the nanogels. By varying the structure of polymers and crosslink density of nanogels, we aim to develop nanogels with tailorable degradation and release profiles under physiological conditions.

2. Experimental Section

2.1. Materials

Glycolide, stannous 2-ethyl hexanoate ($SnOct_2$), 2,2′-azobis(2-methaylpropionitrile) (AIBN), 4,4-azobis(4-cyanopentanoic acid) (ABCPA), hydroxypropyl methacrylate (HEMA), formic acid, 1,1′-carbonyldiimidazole (CDI), 4-(N, N-dimethylamino) pyridine (DMAP), mineral oil (M8410), deuterated dimethyl sulphoxide (DMSO-d_6), perchloric acid ($HClO_4$), and blue dextran (molecular weight 2 000 000 Da) were obtained from Sigma Chemical Co. (St. Louis, MO, USA). Dichloromethane (DCM), hexane, ethyl acetate, methanol, acetonitrile, dimethyl sulphoxide (DMSO, dried over 3 Å molecular sieves), and acetone were purchased from Biosolve (Valkenswaard, The Netherlands). Irgacure 2959 was obtained from Ciba Specialty Chemicals Inc. (Hercules, USA). ABIL EM 90 was provided from Evonik Industries AG (Essen, Germany). HPMAm and HEMAm were synthesized as described previously.[34–36] poly(DL-lactic-co-glycolic acid) (PLGA, PDLG 5004A, Purasorb) was obtained from Corbion, Gorichem, the Netherlands. PLGA nanoparticles with a size of 295 nm as measured by dynamic light scattering (DLS) were prepared using a solvent evaporation method.[37] All other chemicals and solvents were used as received.

2.2. NMR, UPLC, and GPC Analysis of Monomers and Polymers

^{1}H-NMR spectra of the synthesized monomers and polymers dissolved in DMSO-d_6 were recorded with an Agilent 400-NMR spectrometer (Santa Clara, CA, USA). The central line of DMSO at 2.49 ppm was used as reference line.

UPLC analysis of HEMA/HEMAm and HEMA/HEMAm-oligoglycolates was carried out on a Waters ACQUITY UPLC system (Waters Associates Inc., Milford, MA) equipped with an Acquity BEH C18 column 1.7 μm (2.1 × 50 mm) (Waters). The injection volume was 5 μL and the detection wavelength was 210 nm. For the determination of HEMA and HEMA-oligoglycolates, a linear gradient was run from 100% eluent A (10×10^{-3} M $HClO_4$/acetonitrile = 95:5 (v/v)) to 50% eluent B (10×10^{-3} M $HClO_4$/acetonitrile = 5:95 (v/v)) in 1.5 min with a flow rate of 1 mL min^{-1}. For the determination of HEMAm and HEMAm-oligoglycolates, after an isocratic flow of eluent A (10×10^{-3} M $HClO_4$/methanol = 95:5 (v/v)) for 1 min, a gradient was run from 100% eluent A to 50% eluent B (10×10^{-3} M $HClO_4$/methanol = 5:95 (v/v)) in 2 min with a flow rate of 0.5 mL min^{-1} and with detection at 210 nm. The chromatograms were analyzed by Empower Software and the calibration curves of HEMA and HEMAm were linear between 0.02 and 10 μg mL^{-1}.

Molecular weights and molecular weight distributions of the different polymers were determined by Viscotek TDAmax (equipped with RI, light scattering and viscosity detectors, Malvern Instruments Ltd., UK) with a PL aquagel-OH 30 column or a PL aquagel-OH mixed column (Agilent, USA). A 0.3 M sodium acetate buffer (pH 6.5) was used as the eluent with a flow rate of 0.7 mL min^{-1}. Samples were dissolved in the mobile phase and injected onto the column (injection volume 100 μL). Results were analyzed by OmniSEC software (Malvern Instruments Ltd., UK) with poly(ethylene oxide) (M_n: 19 kDa, PDI: 1.04) and pullulan (M_n: 76 kDa, PDI: 1.06) (Malvern Instruments Ltd., UK) as calibration standards.

2.3. Synthesis of HEMA-Oligoglycolates and HEMAm-Oligoglycolates

HEMA-oligoglycolates (HEMA-Gly, containing 1 and 2 glycolate units) and HEMAm-oligoglycolates (HEMAm-Gly, containing 1 to 4 glycolate units) were synthesized via ring opening polymerization.[36] Based on a procedure previously described developed for the synthesis of HPMAm-oligolactates,[38] a mixture of glycolide (2.90 g; 25 mmol) and HEMA (6.50 g, 50 mmol; or HEMAm, 6.45 g, 50 mmol) was melted at 110 °C and stirred under a nitrogen atmosphere. Next, a catalytic amount of $SnOct_2$ (0.20 g, 1 mol% with respect to HEMA or HEMAm; diluted 1:1 with toluene) was added. The reaction mixture was stirred for 1 h at 110 °C and allowed to cool to room temperature. Next, 10 mL of DCM was added to dissolve the products and insoluble compounds were removed by centrifugation (5000 g, 10 min). Next, the supernatant was purified by flash chromatography using a VersaPak silica cartridge (80 mm × 150 mm, 45–75 μm, Sigma-Aldrich) on a VersaFlash chromatography system (Supelco). The mobile phases were hexane/ethyl acetate (80:20, v/v) and DCM/methanol (90:10, v/v) for HEMA-Gly and for HEMAm-Gly, respectively. The flow rate was 80 mL min^{-1}. Fractions that contained HEMA-Gly

or HEMAm-Gly (checked by UPLC analysis) were combined. After evaporation of the solvent, the products were obtained as yellow liquids and characterized by ^{1}H-NMR and UPLC.

2.4. Synthesis of HEMA-Gly-Imidazolyl Carbamate (HEMA-Gly-CI) and HEMAm-Gly-Imidazolyl Carbamate (HEMAm-Gly-CI)

The activation of HEMAm-Gly and HEMA-Gly was conducted according to the procedure published by van Dijk-Wolthuis et al.[39] Basically, CDI (6.4 g, 40 mmol) was dissolved in 50 mL of anhydrous THF and HEMA-Gly (1.7 g, 8 mmol) or HEMAm-Gly (1.9 g, 8 mmol) dissolved in 5 mL of THF was added. The reaction mixture was stirred for 16 h at room temperature. Next, the solution was dropped into 40 mL distilled deionized water to decompose unreacted CDI and shortly shaken until no bubbles (CO_2) were formed. The product in the water/THF phase was extracted with 50 mL DCM for three times and dried on anhydrous $MgSO_4$. After filtration, the solvent was evaporated to yield HEMA-Gly-CI or HEMAm-Gly-CI. The products were characterized by ^{1}H-NMR. The purities (P) of HEMA-Gly-CI and HEMAm-Gly-CI were calculated according to Equation (1)

$$P = \frac{\left(I_{H_a} + I_{H_{a'}}\right)/2 \times M}{\left(I_{H_a} + I_{H_{a'}}\right)/2 \times M + I_{H\,(imidazole)} \times M(\text{imidazole}) + I_{H\,(DCM)}/2 \times M(\text{DCM}) + I_{H(THF)}/2 \times M(\text{THF})} \quad (1)$$

where I_{Ha} and $I_{Ha'}$ are integrals of protons a and a′ in HEMA-Gly-CI or HEMAm-Gly-CI, M is the molecular weight of HEMA-Gly-CI or HEMAm-Gly-CI, $I_{H\,(imidazole)}$ is the integral of the proton at 7.63 ppm, M (imidazole) is the molecular weight of imidazole, $I_{H\,(DCM)}$ is the integral of the protons at 5.73 ppm, M (DCM) is the molecular weight of DCM, $I_{H\,(THF)}$ is the integral of the protons at 1.73 ppm, M (THF) is the molecular weight of THF.

2.5. Synthesis of PolyHPMAm-Gly-HEMA and PolyHEMAm-Gly-HEMAm

pHPMAm and pHEMAm were synthesized by free radical polymerization as follows. For the polymerization of HPMAm, AIBN (230.0 mg, 1.4 mmol) and HPMAm (5.0 g, 35.0 mmol) were dissolved in 25 mL of methanol and transferred into a glass vial. Subsequently, the solution was flushed with N_2 for 30 min., the vial was incubated for 20 h at 60 °C and the obtained polymer was purified by precipitation in diethyl ether for three times (methanol/diethyl ether = 1/40, v/v) and dried in vacuo.

For the synthesis of pHEMAm, ABCPA (725.0 mg, 2.5 mmol) and HEMAm (5.0 g, 37.5 mmol) were dissolved in 200 mL of distilled deionized water, followed for 30 min flushing with N_2. The polymerization was performed at 70 °C for 24 h, after which the solution was transferred into a dialysis tube (molecular weight cutoff 6000 Da) and dialyzed against distilled water for 24 h to remove low molecular weight impurities. pHEMAm was obtained after freeze drying.

The obtained pHPMAm and pHEMAm were characterized by ^{1}H-NMR, and their molecular weights and molecular weight distributions were determined by Viscotek as described in Section 2.2.

To modify the synthesized polymers with HEMA-Gly and HEMAm-Gly, pHPMAm, or pHEMAm (0.8 g) was dissolved in 20 mL of anhydrous DMSO under a nitrogen atmosphere. After dissolution of DMAP (0.16 g), a calculated amount (W) of HEMA-Gly-CI or HEMAm-Gly-CI was added (Equation (2))

$$W = \frac{W_p}{M_m} \times \frac{DS}{100} \times M \times \frac{1}{P} \quad (2)$$

where W_p is the amount of polymer (pHPMAm or pHEMAm), M_m is the molecular weight of the monomer (HPMAm or HEMAm), DS is the degree of substitution (the number of methacryloyl groups per 100 HPMAm or HEMAm units), M is the molecular weight of HEMA-Gly-CI or HEMAm-Gly-CI, and P is the purity of HEMA-Gly-CI or HEMAm-Gly-CI.

The reaction was performed at room temperature for 4 d and terminated by adding 0.16 mL of concentrated HCl to neutralize DMAP and imidazole. The solution was dialyzed against 100×10^{-3} M of ammonium acetate buffer (pH 5) at 4 °C for 2–3 and the polymers were collected after freeze drying. The modified polymers were characterized by ^{1}H-NMR. The DS of final products was measured by quantitative determination of the amount of HEMA or HEMAm formed after incubation of polymers in 0.02 M NaOH at 37 °C for 16 h by UPLC as described in Section 2.2.

2.6. Hydrolysis Kinetics of HEMA-Gly, HEMAm-Gly, pHPMAm-Gly-HEMA, and pHEMAm-Gly-HEMAm

The degradation studies of methacrylic or methacrylamide derivates and modified polymers were performed according to the procedure as described by Neradovic et al.[35] In brief, a 2 mg mL^{-1} solution of HEMA-Gly (or HEMAm-Gly) in DMSO was diluted ten times with phosphate buffer (pH 7.4, 100×10^{-3} M). The solution was incubated at 37 °C. At different time points, samples of 0.2 mL were withdrawn and 0.5 mL of 1 M sodium acetate buffer (pH 4.2) was added to prevent further degradation. The samples were stored at −20 °C before UPLC analysis. Peak areas of HEMA-Gly (or HEMAm-Gly) with different number of glycolate units and HEMA (or HEMAm) in the samples taken at different time points were recorded by UPLC as described in Section 2.2.

To study the hydrolysis of glycolate groups coupled to the polymers, solutions of 20 mg mL^{-1} of pHPMAm-Gly-HEMA (or pHEMAm-Gly-HEMAm) with different DSs in DMSO were diluted ten times with pH 7.4 phosphate buffer (100×10^{-3} M). The samples were incubated at 37 °C and at different time points, samples of 0.2 mL were withdrawn, mixed with 0.5 mL of 1 M sodium acetate buffer (pH 4.2) and stored at −20 °C. HEMA-Gly and HEMA (or HEMAm-Gly and HEMAm) released from the polymers during hydrolysis were determined by UPLC and peak areas were recorded.

2.7. Preparation of Empty and Blue Dextran Loaded Polymeric Nanogels

The preparation of empty polymeric nanogels was based on a mini-emulsion photopolymerization method as described by Raemdock et al.[35] In detail, 37.5 mg of different polymers was dissolved in 412.5 μL of DMSO. Subsequently, Irgacure 2959 (150 μL, 10 mg mL^{-1} in distilled water) was added. This polymer solution (internal phase) was added to 5 mL of mineral oil (light oil, Sigma) containing 10% ABIL EM 90 (v/v) (external phase) and emulsification was carried out by ultrasonication (Labsonic Tip Sonifier, pulse on/off 0.5 s, and amplitude 60%) for 10 min. Next the emulsion was irradiated under UV (60% amplitude, 940 mW cm^{-2}, 300–650 nm, Bluepoint UV source, Honle UV technology, German) for 30 min. Subsequently, the emulsion was mixed with 40 mL of acetone and centrifuged (3000 g, 3 min). The obtained pellet was washed with acetone/hexane (1:1, v/v) for three times, dispersed in 2 mL of distilled water and lyophilized.

To prepare blue dextran loaded nanogels, 5 mg of blue dextran was dissolved in the internal phase and mixed with the external phase. After sonication, irradiation and purification, nanogels were dispersed in a sodium acetate buffer (100×10^{-3} M, pH 5.0). The nonentrapped blue dextran was removed by ultracentrifugation (200 000 g for 30 min). The blue dextran loaded nanogels were obtained after lyophilization.

2.8. Characterization of Polymeric Nanogels

Freeze-dried nanogels were suspended in distilled deionized water, and the size and size distribution were determined by dynamic light scattering (DLS, Malvern ALV/CGS-3 Goniometer, Malvern, UK) at 25 °C.

The zeta potential of nanogels was measured in 20×10^{-3} M HEPES (pH 7.4) by a Malvern Zetasizer Nano-Z (Malvern Instruments, Malvern, UK) at 37 °C.

To determine the conversion of methacrylate/methacrylamide units after photopolymerization, freeze-dried nanogels were dispersed in 0.02 M NaOH (concentration of 1 mg mL^{-1}) and incubated at 37 °C overnight.[41] Subsequently, 0.2 mL sample was withdrawn and mixed with 0.5 mL of sodium acetate buffer (1 M, pH 4.2). UPLC was used to determine the amount of unreacted HEMA/HEMAm (see Section 2.2).

The amount of blue dextran loaded in the nanogels was determined by UV spectrophotometer (UV 2450, Shimadzu, Japan). Nanogels were dispersed in 0.2 M NaOH solution at a concentration of 5 mg mL^{-1} and incubated at 37 °C for 24 h to hydrolyze the nanogels. The concentration of dissolved blue dextran was measured at 620 nm using a calibration curve of blue dextran (linear between 100 and 1000 μg mL^{-1}). Encapsulation efficiency (EE) and loading capacity (LC) were calculated as Equations (3) and (4)

$$\mathrm{EE} = \frac{\text{concentration of blue dextran measured}}{\text{concentration of blue dextran added}} \times 100\% \quad (3)$$

$$\mathrm{LC} = \frac{\text{concentration of blue dextran measured}}{\text{concentration of blue dextran loaded nanogels}} \times 100\% \quad (4)$$

The size and morphology of nanogels were studied by transmission electron microscopy (TEM, Tecnai 10, Philips, 100 kV). Fifteen microliter of nanogel suspension was pipetted onto parafilm. Then, a glow discharged grid was placed on the droplet for 2 min. After removing the excess liquid by a filter paper, the grid was put on a solution of 15 μL of 2% uranyl acetate in water for another 2 min and the excess of uranyl acetate was removed using filter paper. The grid was dried at room temperature for 10 min and loaded into the TEM.

2.9. In Vitro Degradation of Polymeric Nanogels

2.9.1. Dynamic Light Scattering

Polymeric nanogels were dispersed in phosphate buffered saline (PBS, pH 7.4, containing 0.049 M NaH2PO4, 0.099 M Na2HPO4, 0.006 M NaCl) or 100×10^{-3} M sodium acetate buffer (pH 5.0) with the concentration of 0.5 mg mL^{-1} and transferred into a 4 mL cuvette. The samples were incubated at 37 °C and the scattering intensity and particle size were detected at 10 min interval for 48 h. A similar 3 h DLS analysis of DS 20 pHEMAm-Gly-HEMAm nanogels dispersed in sodium tetraborate buffer (100×10^{-3} M, pH 9.0) at 37 °C was performed to accelerate the hydrolytic degradation of the nanogel particles.

2.9.2. Nanoparticle Tracking Analysis

Nanoparticle Tracking Analysis (NTA) was used to size and count the nanogels using a Nanosight LM14 (Malvern Instruments Ltd., UK) with a sample chamber equipped with a 640 nm laser. The nanogel samples, which were taken at different time points from the nanogel suspension incubated at 37 °C in PBS, were diluted 500 times with sodium acetate buffer (100×10^{-3} M, pH 5.0) and introduced into the sample chamber. The data were analyzed by software NTA 3.0 and particle concentration and size distribution were recorded.

2.9.3. Transmission Electron Microscopy

pHEMAm-Gly-HEMAm (DS 5) nanogels were dispersed in 20×10^{-3} M HEPES (pH 7.4) and incubated at 37 °C. At 0, 2, 6, 24 h, samples were taken and stained with 2% uranyl acetate, and observed with TEM. The same nanogel dispersion incubated in pH 5.0 HEPES buffer (20×10^{-3} M) for 24 h was analyzed as well.

2.9.4. Characterization of Nanogel Soluble Degradation Products

The structure, amount and molecular weight of the water-soluble polymers that were formed during degradation of nanogels were determined by ^{1}H-NMR and Viscotek. Briefly, nanogel suspensions (5 mg mL^{-1}, 5 mL) in PBS buffer or 0.02 M NaOH were incubated at 37 °C. At different time points, 200 μL samples were taken and the pH was adjusted to 5.0 by 0.1 M HCl (20 μL for PBS and 14 μL for 0.02 M NaOH). After centrifugation (22 000 g, 120 min), the supernatant was analyzed by Viscotek as described in Section 2.2. The normalized amount of formed soluble polymer was calculated by dividing the concentration of polymer measured by Viscotek by the initial concentration of nanogel suspension. The water-soluble polymer present in the supernatant after incubation of DS 5 pHEMAm-Gly-HEMAm nanogels for 16 h in

0.02 M NaOH was characterized by ^{1}H-NMR (see Section 2.2, using DMSO-d_6 as the solvent).

2.10. In Vitro Release of Blue Dextran

To study the release of blue dextran, nanogels were suspended in 100 × 10^{-3} M phosphate buffer (pH 7.4) at a concentration of 10 mg mL^{-1} and incubated at 37 °C. At different time points, 100 μL samples were taken and mixed with 100 μL of 1 M sodium acetate buffer (pH 5.0) to prevent further degradation. The mixture was centrifuged at 22 000 g for 120 min and the absorbance of the supernatant was determined at 620 nm.

2.11. Cytocompatibility Studies

2.11.1. Cell Culture

HUVEC (human umbilical vein endothelial) cells were obtained from human umbilical cords and cultured in EBM-2 medium supplemented with EGM-2 kit (Lonza, USA). RAW 264.7 macrophage cells were cultured in DMEM (Sigma, USA), supplemented with 10% fetal bovine serum (FBS) (Invitrogen, Germany). Cell lines were kept at 37 °C and 5% CO_2, in a humidified atmosphere.

2.11.2. MTS Assay

The cell viabilities upon incubation with pHEMAm-Gly-HEMAm nanogels with different DSs were evaluated via the MTS assay and using PLGA nanoparticles as positive control. 12 000 HUVECs per well and 10 000 RAW 264.7 cells per well were seeded into 96-wells plates. After 24 h, the medium was removed and 200 μL of pHEMAm-Gly-HEMAm nanogel or PLGA nanoparticle dispersions in medium was added to the wells at a concentration ranging from 0.0325 to 2 mg mL^{-1}. After 24 h of incubation, the MTS assay (Promega, USA) was performed by pipetting 40 μL of MTS reagent into each well. The plate was incubated at 37 °C for 2 h in a humidified, 5% CO_2 atmosphere. Finally the absorbance at 492 nm was recorded using a reference wavelength of 690 nm.

2.11.3. LDH Leakage Assay

The leakage of lactate dehydrogenase (LDH), a cytosolic enzyme, upon cell lysis during incubation of pHEMAm-Gly-HEMAm nanogels and PLGA nanoparticles was measured using an assay that measures the activity of the enzyme. In detail, HUVEC cells or RAW 264.7 cells were seeded into a 96-well plate at the density of 12 000 or 10 000 cells per well, respectively. After incubation at 37 °C for 2 h in a humidified, 5% CO_2 atmosphere, the medium was removed and 200 μL of nanogels or nanoparticle samples in medium was added to the wells at the concentration from 0.0325 to 2 mg mL^{-1}. After 24 h incubation, LDH assay was performed according to manufacturer's protocol (Promega, USA). To generate a maximum of LDH release, 20 μL of 10× Lysis Solution was added to untreated cells which were subsequently incubated for 45 min. Subsequently, 50 μL aliquots from the wells were transferred into a 96-well plate, followed by addition of the LDH reagent. Next, the plate was incubated at room temperature in the dark. After 30 min, 50 μL of stop solution was added to the wells and the absorbance at 492 nm was recorded with reference wavelength of 690 nm. The relative LDH leakage (%) was calculated as Equation (5)

$$\text{Relative LDH leakage } (\%) = \frac{OD_{sample} - OD_{background}}{OD_{maximum} - OD_{background}} \times 100\% \quad (5)$$

where OD_{sample} is the absorbance of the test sample, $OD_{maximum}$ is the absorbance of LDH release from cells incubated with the lysis buffer and $OD_{background}$ is the absorbance of medium.

3. Results and Discussion

This study describes the rational design of polymeric nanogels with tailorable degradation behavior under physiological conditions, potentially suitable for drug delivery purposes. To this end, two water-soluble biocompatible and nontoxic polymers, pHPMAm and pHEMAm, were synthesized and used as building blocks for nanogels. These polymers were subsequently modified with polymerizable methacrylate or methacrylamide groups which contain glycolate esters as biodegradable bonds (HEMA-Gly or HEMAm-Gly (see Figure 1A)), respectively. The degradation profiles of nanogels prepared from polymers with different structures and crosslink densities were studied (Figure 1B).

3.1. Synthesis of HEMA/HEMAm-Oligoglycolates

The synthesis of HEMA-oligoglycolates (HEMA-Gly) and HEMAm-oligoglycolates (HEMAm-Gly) was done by ring-opening polymerization of glycolide initiated by HEMA/HEMAm using $SnOct_2$ as the catalyst. As demonstrated in previous studies for comparable reactions,[39] the average degree of polymerization of HEMA(m)-oligoglycolates could be controlled by the feed ratio of HEMA(m) and glycolide. Considering the poor water-solubility of products with relatively long oligoglycolate chains, which in turn will adversely affect the hydrophilicity of the final nanogels, we chose a HEMA(m)/glycolide ratio of 2:1 (mol/mol) aiming at a low degree of polymerization. After 1 h reaction, the crude product was purified by flash chromatography. HEMAm-Gly was more difficult to separate in different fractions than HEMA-Gly. Therefore, fractions containing HEMA-Gly (with 1 to 2 glycolate units) or HEMAm-Gly (with 1 to 4 glycolate untis) were combined. UPLC chromatograms (Figure S1, Supporting Information) show that both products had less than 3% of unreacted HEMA or HEMAm. Yields of HEMA-Gly and HEMAm-Gly were 27% and 48%, respectively. The average degrees of polymerization (DP; determined by ^{1}H-NMR) of HEMA-Gly and HEMAm-Gly were 1.46 and 1.84, respectively.

^{1}H-NMR HEMA-Gly (Figure S2A (Supporting Information), DMSO-d_6, 400 MHz): δ 6.09 (s, 1H, H_a), 5.57 (s, 1H,

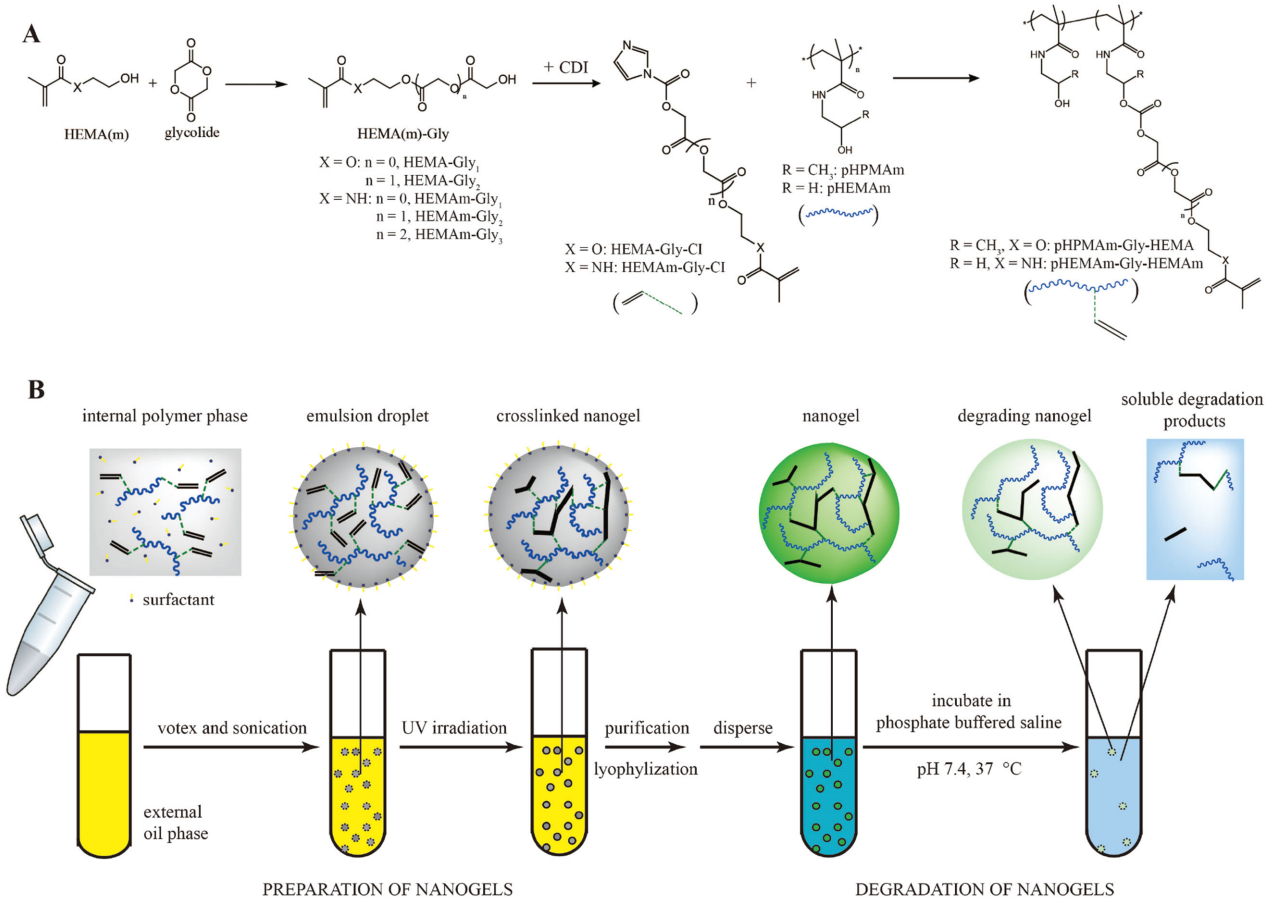

Figure 1. Biodegradable polymeric nanogels based on pHPMAm-Gly-HEMA or pHEMAm-Gly-HEMAm. A) Synthesis of pHPMAm-Gly-HEMA or pHEMAm-Gly-HEMAm. B) Preparation and degradation of nanogels.

$H_{a'}$), 4.71 (m, 2H, H_e), 4.42–4.27 (m, 4H, H_c, H_d), 4.16 (m, 2H, H_f), 1.91 (s, 3H, H_b).

^{1}H-NMR HEMAm-Gly (Figure S2B (Supporting Information), DMSO-d_6, 400 MHz): δ 8.01 (m, 1H, H_c), 5.63 (s, 1H, H_a), 5.32 (s, 1H, $H_{a'}$), 4.88–4.63 (m, 2H, H_f), 4.14–3.99 (m, 4H, H_e, H_g), 3.30 (m, 2H, H_d), 1.83 (s, 3H, H_b).

3.2. Synthesis of HEMA-Gly-CI and HEMAm-Gly-CI

To couple HEMA-Gly (or HEMAm-Gly) to pHPMAm (or pHEMAm), CDI was used to activate the hydroxyl group of the glycolates. An excess CDI (molar ratio of CDI and hydroxyl groups: 5:1) was added to activate HEMA-Gly (or HEMAm-Gly) completely and to avoid the formation of HEMA-Gly-HEMA (or HEMAm-Gly-HEMAm).[39] Next, unreacted CDI was decomposed with water and once bubbles (CO_2 produced by the reaction of CDI and water) were not formed anymore, HEMA-Gly-CI (or HEMAm-Gly-CI) was extracted with DCM.

The ^{1}H-NMR spectra of HEMAm-Gly-CI before (Figure S3A, Supporting Information) and after (Figure S3B, Supporting Information) purification show that CDI was indeed removed. Comparison of Figure S2B with Figure S3B (Supporting Information) shows that there is a shift of the terminal glycolate proton (H_g) of HEMAm-Gly from 4.14 to 5.15 ppm, and the imidazole signals appear at 7.58 and 7.11 ppm. The yields of HEMA-Gly-CI and HEMAm-Gly-CI were 92% and 95%, respectively. The purities (P) of HEMA-Gly-CI and HEMAm-Gly-CI were 62% and 43% respectively according to NMR analysis (Equation (1)). One of the main impurities that remain in the final product is imidazole. Since it has been shown previously that this compound does not affect the reaction of activated side units of HEMA(m)-Gly-CI and polymers in DMSO,[39] HEMA-Gly-CI (or HEMAm-Gly-CI) together with imidazole was used for further reaction.

^{1}H-NMR HEMA-Gly-CI (Figure S3C (Supporting Information), DMSO-d_6, 400 MHz): δ 8.15 (s, 1H, H_g), 7.42 (s, 1H, H_i), 7.08 (s, 1H, H_h), 6.07 (s, 1H, H_a), 5.56 (s, 1H, $H_{a'}$), 4.98–4.63 (m, 4H, H_e, H_f), 4.48–4.30 (m, 4H, H_c, H_d), 1.90 (s, 3H, H_b).

^{1}H-NMR HEMAm-Gly-CI (Figure S3B (Supporting Information), DMSO-d_6, 400 MHz): δ 8.16 (m, 1H, H_c), 7.58 (s, 1H, H_h), 7.11 (m, 2H, H_i, H_j), 5.63 (s, 1H, H_a), 5.31 (s, 1H, $H_{a'}$),

5.15–4.89 (m, 4 H, H_f, H_g), 4.2 (m, 2H, H_e), 3.36 (m, 2H, H_d), 1.82 (s, 3H, H_b).

3.3. Synthesis of pHPMAm-Gly-HEMA and pHEMAm-Gly-HEMAm

pHPMAm and pHEMAm were obtained by free radical polymerization. Due to its high hydrophilicity and poor solubility in methanol, unlike the polymerization of HPMAm in methanol, the synthesis of pHEMAm was performed in water using ABCPA as initiator. The reaction conditions were chosen to synthesize polymers with a number average molecular weight less than 20 kDa (pHPMAm: M_n 17.3 kDa, PDI 2.20; pHEMAm: M_n 15.9 kDa, PDI 2.20) because pHPMAm with molecular weight <45 kDa can be cleared by the kidneys.[41–43]

Methacrylated polymers were obtained by coupling HEMA-Gly-CI and HEMAm-Gly-CI to pHPMAm and pHEMAm. The ^{1}H-NMR spectrum of pHEMAm-Gly-HEMAm shows that HEMAm-Gly was indeed successfully coupled to pHEMAm (Figure S4, Supporting Information). pHPMAm-Gly-HEMA (DS 4 and 8) and pHEMAm-Gly-HEMAm (DS 5, 8, and 20) were synthesized to investigate the effect of DS, and thus crosslink density, on the degradation behavior of the prepared nanogels.

3.4. Hydrolytic Degradation Study of Monomers and Polymers

The degradation of the nanogels is due the hydrolysis of carbonate esters and glycolate esters in the crosslinks of polymer networks. Therefore, to get insight into the degradation mechanism and kinetics of the nanogels, the hydrolysis kinetics of HEMA-Gly (and HEMAm-Gly) and pHPMAm-Gly-HEMA (and pHEMAm-Gly-HEMAm) was studied at pH 7.4 and at 37 °C. A high salt concentration (100×10^{-3} M) of the buffer solution was used to maintain the pH during the incubation and a cosolvent (10% DMSO) was used to fully solubilize the monomers and polymers.

3.4.1. Hydrolysis of Monomers

Figure S5A (Supporting Information) shows the chromatograms of HEMA-Gly upon incubation at pH 7.4 and 37 °C. As anticipated, HPLC analysis showed that HEMA-Gly_1 (HEMA-Gly with one glycolate unit) and HEMA-Gly_2 (HEMA-Gly with two glycolate units) were converted into HEMA, which was further slowly converted into MA. The chromatograms of HEMAm-Gly degradation samples (Figure S5B, Supporting Information) show that the peak areas of HEMAm-Gly decreased in time, which was associated with a concomitant increase of HEMAm. The linearity obtained by plotting the natural logarithm of the concentration of HEMA(m)-Gly_1 and HEMA(m)-Gly_2 versus time (Figure 2) demonstrates that the hydrolysis of ester bonds in these compounds follows pseudo-first-order kinetics. The hydrolysis rate constants of ester bonds in HEMA(m)-Gly were calculated from the ln area versus time plots (Figure S6, Supporting Information) and reported in Table 1. The detailed calculation is described in the Supporting Information.

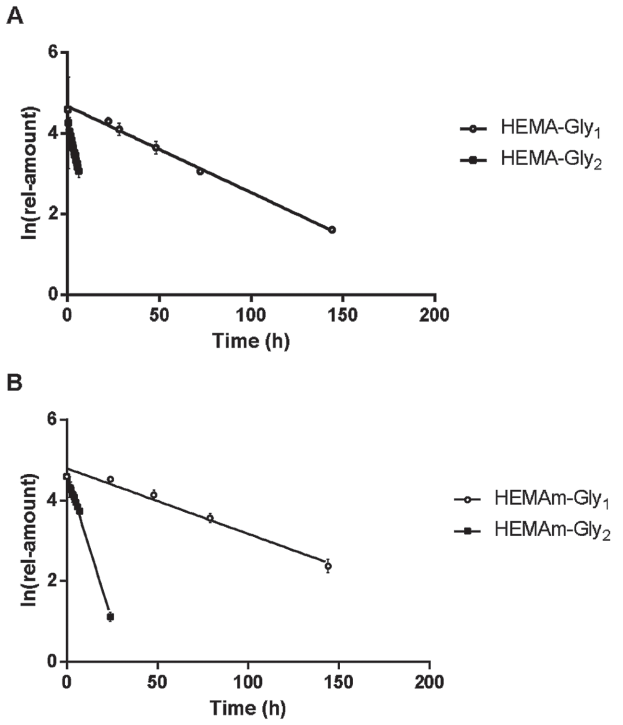

Figure 2. Natural logarithm of the relative amounts (% with respect to the amounts at $t = 0$) of A) HEMA-Gly and B) HEMAm-Gly during degradation at 37 °C in 100×10^{-3} M phosphate buffer (pH7.4) containing 10% DMSO, $n = 3$.

As shown in Table 1, the rate of the hydrolysis reaction for HEMA-Gly_2 (k_{bb} = 0.18 h^{-1}) is about ten times faster than the hydrolysis rate of the terminal glycolate ester (k_{Gly} = 0.022 h^{-1}). This rapid hydrolytic degradation of HEMA-Gly_2 can be explained by the formation of a stable six-membered ring (Figure 3A; "backbiting"), as previously suggested for the hydrolysis of oligo(lactic acid) in alkaline enviroment.[45] Table 1 furthers shows that k_{bb} for HEMA-Gly_2 (0.18 h^{-1}) is greater than that of the previously reported value for HPMAm-$lactate_2$ (0.14 h^{-1}).[35] This can be explained by the faster hydrolysis of an ester of a primary alcohol (glycolate ester) than an ester of a secondary alcohol (lactate ester). The rate constant of conversion from HEMA to MA (k_{MA} = 0.00043 h^{-1}) is similar as reported previously (0.00036 h^{-1}).[45] No methacrylic acid was detected as degradation product of HEMAm-Gly which can be explained by the high stability of the amide bond under the selected condition.[35]

Table 1. Hydrolysis rate constants of HEMA(m)-Gly ($n = 3$) at 37 °C and at pH 7.4.

Monomers	k_{HEMAm} [a)] [h^{-1}]	k_{Gly} [b)] [h^{-1}]	k_{bb} [c)] [h^{-1}]
HEMA-Gly_1	–	0.022 ± 0.001	–
HEMA-Gly_2	–	0.022 ± 0.001	0.18 ± 0.01
HEMAm-Gly_1	0.027 ± 0.003	–	–
HEMAm-Gly_2	–	0.098 ± 0.007	0.068 ± 0.003
HEMAm-Gly_3	0.027 ± 0.001	0.098 ± 0.008	≈3

[a)]k_{HEMAm} refers to the hydrolysis constant of the ester bond between HEMAm and glycolic acid (see Figure 3); [b)]k_{Gly} refers to the hydrolysis constant of the glycolate ester bond; [c)]k_{bb} refers to the rate constant of the backbiting reaction.

The k_{Gly} of HEMAm-Gly_1 is almost equal to that of HEMA-Gly_1 (0.027 h^{-1} vs 0.022 h^{-1}). However, Table 1 shows a five times faster hydrolysis of the terminal glycolate ester in HEMAm-Gly_2 than in HEMA-Gly_2 (0.098 h^{-1} vs 0.022 h^{-1}). This can be explained by the formation of an intramolecular hydrogen bond between the amide and the terminal carbonyl group via a 10 ring. The increased electrophilicity of the terminal carbonyl group caused by this hydrogen bridge formation makes attack of a water molecule at that site energetically more favorable (Figure 3B). Therefore, the hydrolysis rate constant of the terminal glycolate ester in HEMAm-Gly_2 is higher than that in HEMAm-Gly_1 which is not able to form an intramolecular hydrogen bridge with the amide group via a 10 ring. Further, a four times slower backbiting rate constant is observed (Table 1) for HEMAm-Gly_2 than for HEMA-Gly_2 (0.068 h^{-1} vs 0.18 h^{-1}). This can be explained by the formation of another intramolecular hydrogen bond between the second carbonyl group and the hydroxyl group via an 8 ring in HEMAm-Gly_2 (Figure 3B). The hydrogen bond reduces the chance of nucleophilic attack of the hydroxyl end group on the second carbonyl group present in HEMA-Gly_2. This hypothesis is confirmed by the surprisingly high degradation rate constant of backbiting in HEMAm-Gly_3 (40 times faster than backbiting in HEMAm-Gly_2). The intramolecular hydrogen bridge formation between the amide and the third carbonyl group (Figure 3B) increases the electrophilicity of the carbon of the third carbonyl group. This makes the nucleophilic attack of the hydroxyl end group on the third carbonyl group energetically more favorable (Figure 3B).

3.4.2. Hydrolysis of the Polymers

The degradation profiles of pHPMAm-Gly-HEMA at 37 °C and pH 7.4 is shown in Figures S7A and S8 (Supporting Information). These figures show that the amounts of HEMA and MA continuously increased in time, whereas the amount of HEMA-Gly_1 first increased and then decreased after having reached at maximum at 8 h. This indicates that during hydrolysis, the products that are split from the polymer backbone (i.e., HEMA, HEMA-Gly_1, and HEMA-Gly_2) are further degraded, in line with the data of hydrolysis of HEMA-Gly (Section 3.4.1). A similar pattern is found for the degradation of pHEMAm-Gly-HEMAm (Figures S7B and S9, Supporting Information).

Since there are two types of ester bonds present in the polymer, i.e., carbonate and glycolate ester, two new rate constants ($k_{carbonate}$ and $k_{Gly\text{-}p}$) are introduced to describe the hydrolysis of these two ester bonds (Figure 4, pHPMAm/pHEMAm and pHPMAm-glycolic acid /pHEMAm-glycolic acid are formed, respectively).

Figure S10 (Supporting Information) shows that for pHPMAm-Gly-HEMA, $k = 0.022$ h^{-1} which value is the same as for k_{Gly} (Table 1). Furthermore, HEMA-Gly_2 was hardly detected which can be explained by the relatively high rate constant for the backbiting reaction (k_{bb} = 0.18 h^{-1}) as soon as this compound is formed.

For pHEMAm-Gly-HEMAm, the rate constant for the hydrolysis of the glycolate ester bond in formed HEMAm-Gly_1 to yield HEMAm is 0.026 h^{-1} (Figure S11, Supporting Information). This value is very close to the k_{HEMAm} of HEMAm-Gly as reported in Table 1 (k = 0.027 h^{-1}). Compared to pHPMAm-Gly-HEMA, the hydrolysis of the carbonate ester of pHEMAm-Gly-HEMAm is faster (Table 2, 0.034 h^{-1} vs 0.047 h^{-1} for DS 8 polymers). Less steric hindrance in pHEMAm-Gly-HEMAm due to the absence of a methyl group next to the carbonate group can explain this difference. Furthermore, a greater $k_{Gly\text{-}p}$ is found for pHEMAm-Gly-HEMAm than for pHPMAm-Gly-HEMA (Table 2, 0.085 h^{-1} vs 0.063 h^{-1} for DS 8 polymer). This can be explained by the formation of an intramolecular hydrogen bond between the amide and the carbonyl group next to the carbonate ester via a 10 ring in the side group resulting in an increased electrophilicity of the carbonyl which makes an attack of a water molecule more favorable (Figure S12, Supporting Information), as also suggested for the hydrolysis of HEMAm-Gly (Figure 3).

It should be noted that there is no significant influence of DS of the polymers on the hydrolysis rate. That is because the average distance between two side groups is 5 HEMAm units for DS 20 polymer, meaning that these

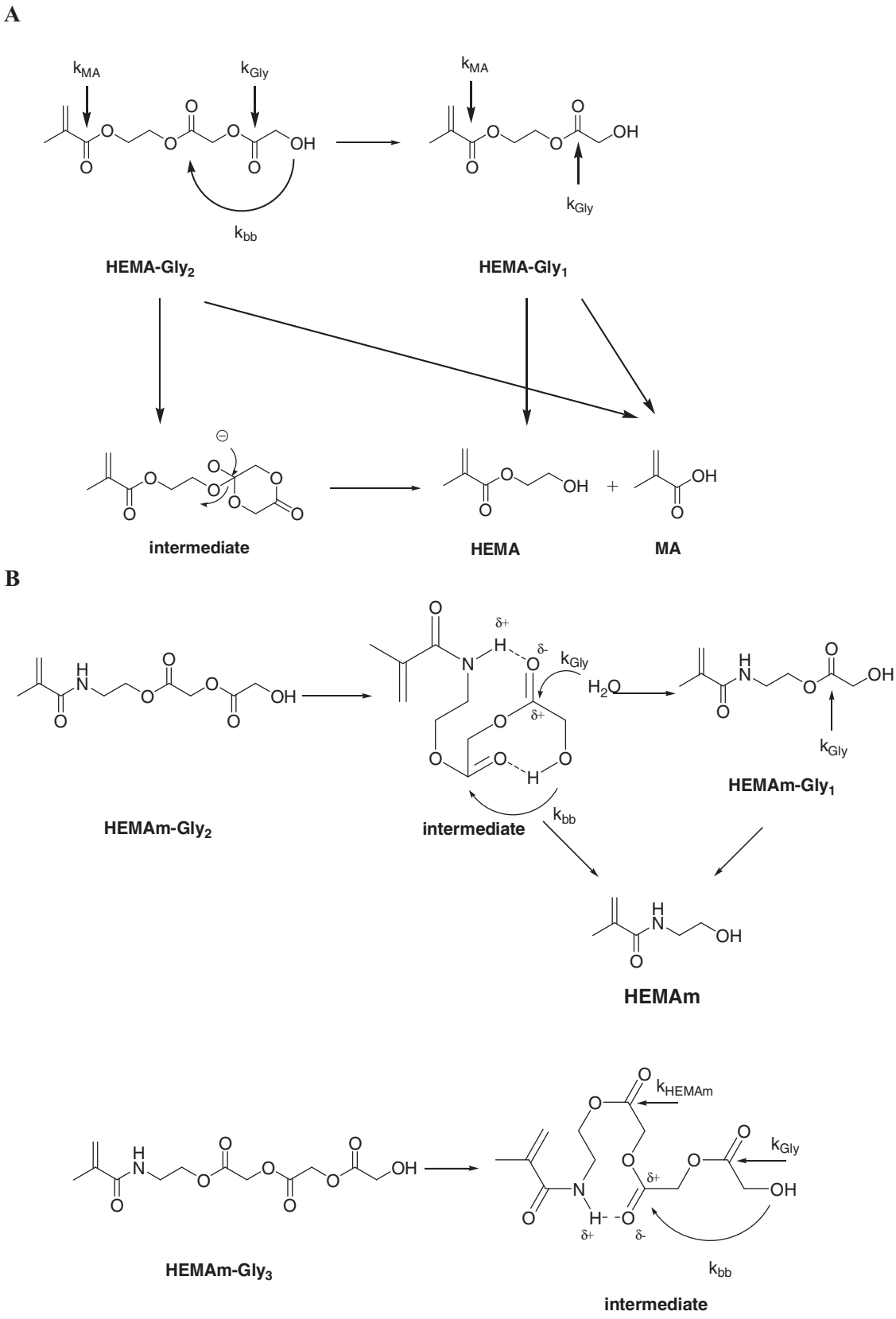

Figure 3. Possible hydrolysis routes of A) HEMA-Gly and B) HEMAm-Gly.

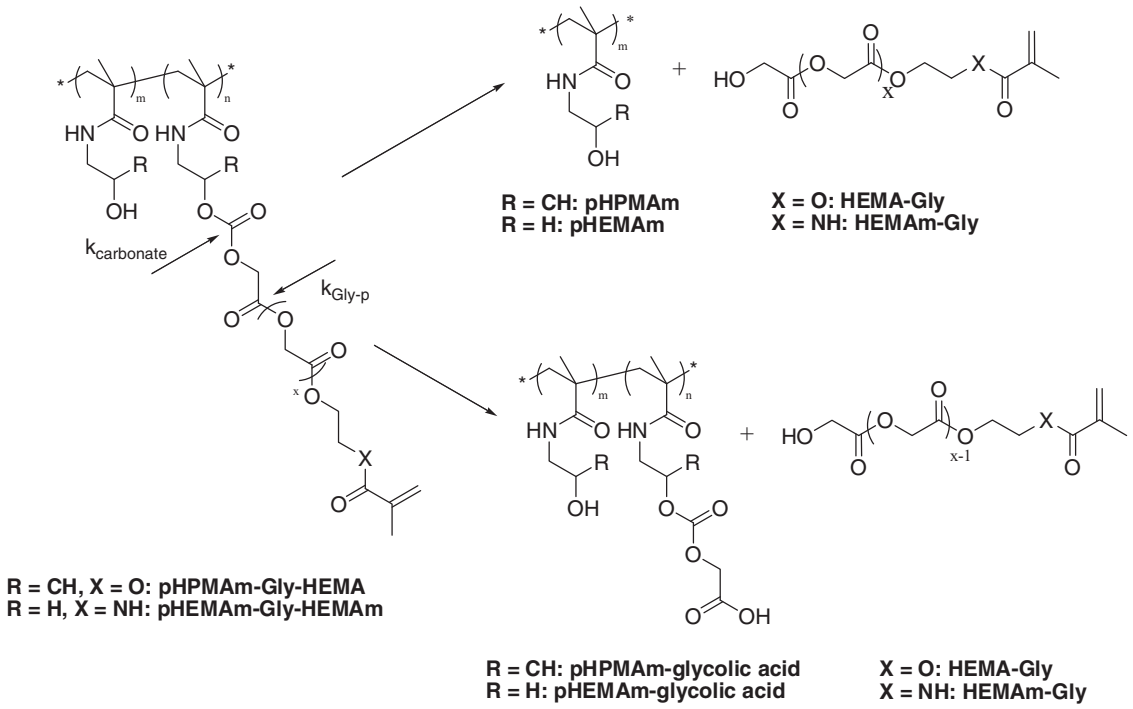

Figure 4. Hydrolysis sites and reactions of pHPMAm-Gly-HEMA and pHEMAm-Gly-HEMAm.

groups do not "see" each other resulting in equal hydrolytic reaction rates.[45]

3.5. Preparation and Characterization of Nanogels

Inverse emulsion photopolymerization was selected as method to prepare nanogels following a literature procedure with some modifications.[46] A solution of polymers in DMSO was used as the internal phase, whereas mineral oil together with the surfactant ABIL EM 90 was the external phase. An emulsion was created by sonication in an ice-water bath to minimize hydrolysis of glycolate side units by water used to dissolve the photoinitiator. Next, the emulsion was UV irradiated for 30 min, which resulted in almost complete conversion of methacrylate groups (>90%, Table 3). After photopolymerization, the particles were washed and obtained after freeze drying in a good yield (>80%). DLS showed the diameters of particles after dispersion in water were around 130–160 nm with small size distribution (PDI < 0.2); the zeta potential of the nanogels in HEPES buffer (pH 7.4) was neutral. These nanogels have a similar size because the same concentration of polymers in the internal phase was used for nanogel preparation. Therefore, it is in the line with expectation that the size of particles is similar for the different batches. TEM analysis showed spherical particles with size 50–100 nm (Figure 5A). Compared with TEM results, DLS analysis gave a bigger size hydrated particles were used, whereas TEM analysis was done on dried samples.

To prepare blue dextran loaded nanogels, this macromolecule was dissolved in the internal phase and other steps were the same as for the preparation of empty nanogels. The size of loaded nanogels was slight bigger than those of the empty nanogels (Tables 3 and 4). Table 4 also shows the blue dextran was loaded with a high efficiency in the nanogels (≈70%–85%).

Table 2. Hydrolysis rate constants of pHPMAm-Gly-HEMA and pHEMAm-Gly-HEMAm at 37 °C in 100×10^{-3} M phosphate buffer (pH 7.4, containing 10% DMSO), $n = 3$.

Polymers	$k_{carbonate}$ [a] $[h^{-1}]$	k_{Gly-p} [b] $[h^{-1}]$
pHPMAm-Gly-HEMA DS 4	0.032 ± 0.001	0.058 ± 0.002
pHPMAm-Gly-HEMA DS 8	0.034 ± 0.002	0.063 ± 0.002
pHEMAm-Gly-HEMAm DS 5	0.048 ± 0.003	0.087 ± 0.004
pHEMAm-Gly-HEMAm DS 8	0.047 ± 0.002	0.085 ± 0.003
pHEMAm-Gly-HEMAm DS 20	0.048 ± 0.002	0.087 ± 0.004

[a] $k_{carbonate}$ refers to the rate constant for the hydrolysis of the carbonate ester bond; [b] k_{Gly-p} refers to the rate constant for the hydrolysis of the glycolate ester bond (see Figure 4).

3.6. Degradation of Nanogels

3.6.1. DLS

Degradation of yielded nanogels was studied in PBS (pH 7.4) at 37 °C. DLS was used to measure changes in scattering

Table 3. Characteristics of empty nanogels ($n = 3$) prepared using polymers with different degrees of substitution.

Polymers	Yield [%][a)]	Size [nm]	PDI	Conversion [%][b)]	Zeta potential [mV]
pHPMA-Gly-HEMA DS 4	97.0 ± 0.9	137.4 ± 5.2	0.16 ± 0.02	90.3 ± 3.4	–0.23 ± 0.00
pHPMA-Gly-HEMA DS 8	91.8 ± 3.2	168.6 ± 6.2	0.23 ± 0.01	91.4 ± 3.2	–0.56 ± 0.01
pHEMAm-Gly-HEMAm DS 5	96.2 ± 2.5	137.1 ± 5.9	0.26 ± 0.02	94.6 ± 2.2	–1.01 ± 0.02
pHEMAm-Gly-HEMAm DS 8	86.4 ± 3.1	131.3 ± 8.4	0.22 ± 0.01	95.4 ± 2.8	–0.91 ± 0.01
pHEMAm-Gly-HEMAm DS 20	82.1 ± 1.9	129.6 ± 5.2	0.21 ± 0.02	92.6 ± 3.0	–0.98 ± 0.03

[a)]Yield is the ratio of the amount of nanogels obtained after lyophilization and the amount of fed materials; [b)]conversion is the ratio of the amount of unreacted methacrylate groups in nanogels and the total amount of methacrylate groups of the polymers used to prepare the nanogels.

intensity of nanogel suspension as well as in size. As shown in Figure 6, pHEMAm-Gly-HEMAm nanogels have a faster decrease in count rate (i.e., scattering intensity) than pHPMAm-Gly-HEMA nanogels. This observation is in line with the hydrolysis data which show that pHEMAm-Gly-HEMAm is more rapidly hydrolyzed than pHPMAm-Gly-HEMA (Section 3.4.2, Table 2). Figure 6B shows that pHEMAm-Gly-HEMAm nanogels prepared from lower DS polymers display a faster decrease in count rate and thus more rapidly degrade than nanogels prepared from higher DS polymers. Table 2 shows that the hydrolysis rates of the ester bonds of the side groups are independent of DS. However, the crosslink density is lower for nanogels prepared from lower DS polymers and as a consequence fewer crosslinks have to be cleaved for these nanogels to degrade. Furthermore, the size and PDI of nanogels increased during incubation (Figure S13, Supporting Information). Taken DS 5 pHEMAm-Gly-HEMAm nanogels as an example (Figure S13A, Supporting Information) shows that the size increased with 10 nm and PDI increased from 0.2 to 0.4 after 48 h incubation. As a control, pHEMAm-Gly-HEMAm (DS 5) nanogels were incubated in 100×10^{-3} M sodium acetate buffer (pH 5.0) (Figure S14, Supporting Information). Neither a decrease in count rate nor change in size was observed, demonstrating that the glycolate esters and carbonate esters in the crosslinks of nanogels are relatively

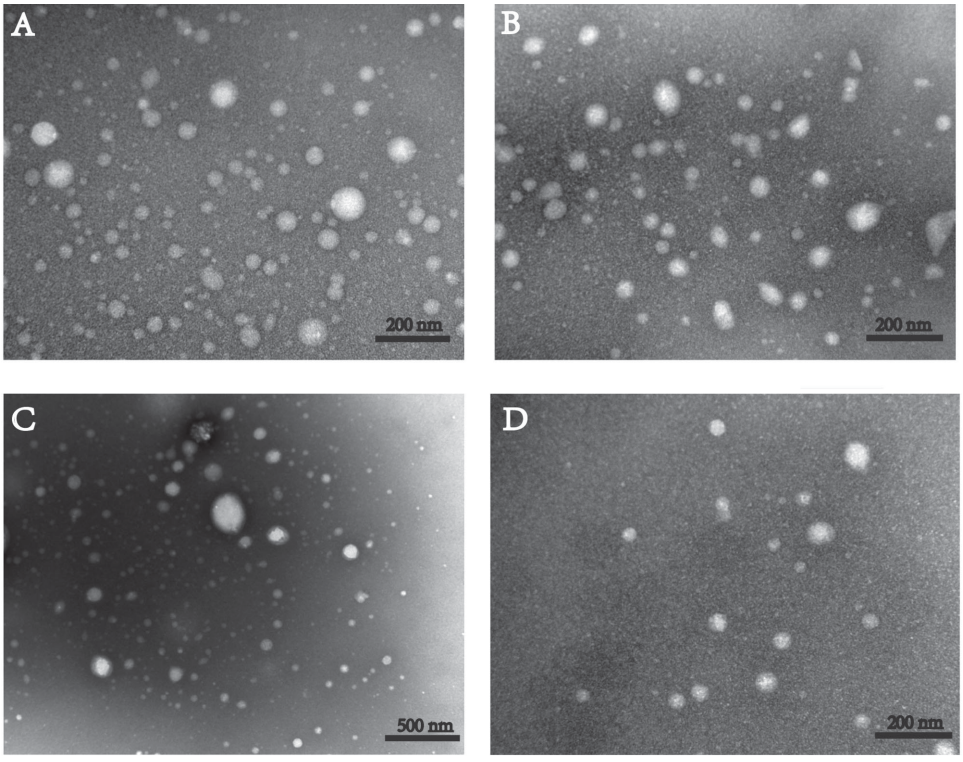

Figure 5. TEM images of pHEMAm-Gly-HEMAm nanogels (DS 5) incubated in 20×10^{-3} M HEPES (pH 7.4) at 37 °C for A) 0 h, B) 2 h, C) 6 h, and in 20×10^{-3} M HEPES (pH 5) at 37 °C for D) 24 h.

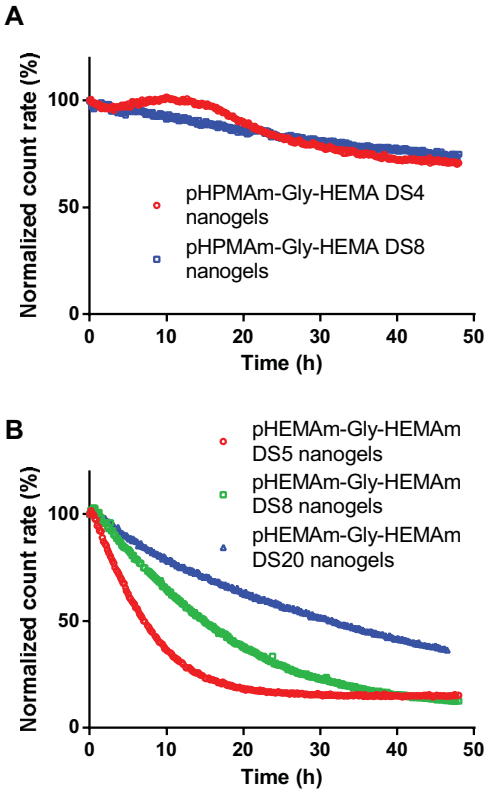

Figure 6. Degradation of nanogels in PBS at 37 °C as function of crosslink density measured by dynamic light scattering: A) pHPMAm-Gly-HEMA nanogels, and B) pHEMAm-Gly-HEMAm nanogels.

stable at pH 5.0.[44,47] At pH 9.0, the count rate of pHEMAm-Gly-HEMAm (DS 20) nanogel suspension decreased about 20 times faster than at pH 7.4 ($t_{1/2}$: 1 h vs 25 h) (Figure S15, Supporting Information), which is in line with faster degradation of glycolate esters and carbonate esters under alkaline conditions.[48] Because of the good tailorability of the degradation behavior of pHEMAm-Gly-HEMAm nanogels (degradation time depends on DS of polymers), they were chosen as a lead for further degradation studies using NTA.

3.6.2. NTA

The count rate (light scattering intensity) as measured by DLS depends on the size, concentration and the water-content (affects the particle-to-medium refractive index ratio or dn/dc value) of the particles[49] and these factors cannot be singled out by the DLS equipment. To investigate the change of each factor separately, NTA was used to study the degradation of nanogels. NTA tracks the Brownian motion of nanoparticles, and the software calculates the size of the particles using the Stokes–Einstein equation as well as the particle concentration.[50] NTA showed that nanogels based on pHEMAm-Gly-HEMAm (DS 5) had a continuous decrease in particle concentration during 48 h incubation in PBS (pH 7.4) at 37 °C (Figure 7A). On the other hand, under the same conditions nanogels based on DS 8 pHEMAm-Gly-HEMAm showed a plateau during the 16 h of incubation after which the concentration decreased in time and about 30% of particles remained after 48 h (Figure 7B). For nanogels based on DS 20 pHEMAm-Gly-HEMAm a plateau was observed for 30 h and thereafter the number of particles in the suspension decreased to 60% of the initial value after 48 h (Figure 7C). Moreover, during the incubation of DS 8 nanogels from 0 to 16 h (the number of particles remains constant) the scattering intensity of particles decreased (Figure S16, Supporting Information), demonstrating that the density of nanogels decreased due to hydrolysis of the crosslinks and as a consequence the dn/dc value decreased. Once the crosslinks were too few to keep particles intact, nanogels started to disassociate and the concentration of particles in the suspension decreased. It is obvious that for nanogels prepared from higher DS polymers more crosslinks have to be hydrolyzed before nanogel disassociation occurs, which leads to a longer plateau (16 h for DS 8 nanogels vs 30 h for DS 20 nanogels). Likely, for DS 5 nanogels the plateau is too short to be observed.

Similar to the DLS results, the size of nanogels measured by NTA increased during incubation (Figure 7). Both DLS and NTA show nanogels with lower crosslink density have faster degradation behavior. Since a plateau in number of particles and increased particle size are observed by NTA (Figure 7B,C), the decrease in count rate measured by DLS (Figure 6B) in the early stage of incubation is because of the decrease of the dn/dc value instead of the decrease of nanogel concentration. The figures mentioned above (Figures 6B, Figure 7B,C) also show that after the plateau the decrease of count rate is due to the decrease of the dn/dc as well as the concentration.

Table 4. Characteristics of blue dextran loaded nanogels ($n = 3$).

Polymers	Size [nm]	PDI	EE [%][a)]	LC [%][b)]
pHEMAm-Gly-HEMAm DS 5	170.3 ± 2.0	0.20 ± 0.01	70.0 ± 0.3	8.57 ± 0.06
pHEMAm-Gly-HEMAm DS 8	168.6 ± 2.6	0.21 ± 0.02	84.7 ± 0.2	10.17 ± 0.06
pHEMAm-Gly-HEMAm DS 20	165.9 ± 1.3	0.21 ± 0.03	86.5 ± 0.2	10.37 ± 0.06

[a)]EE refers to encapsulation efficiency; [b)]LC refers to loading capacity.

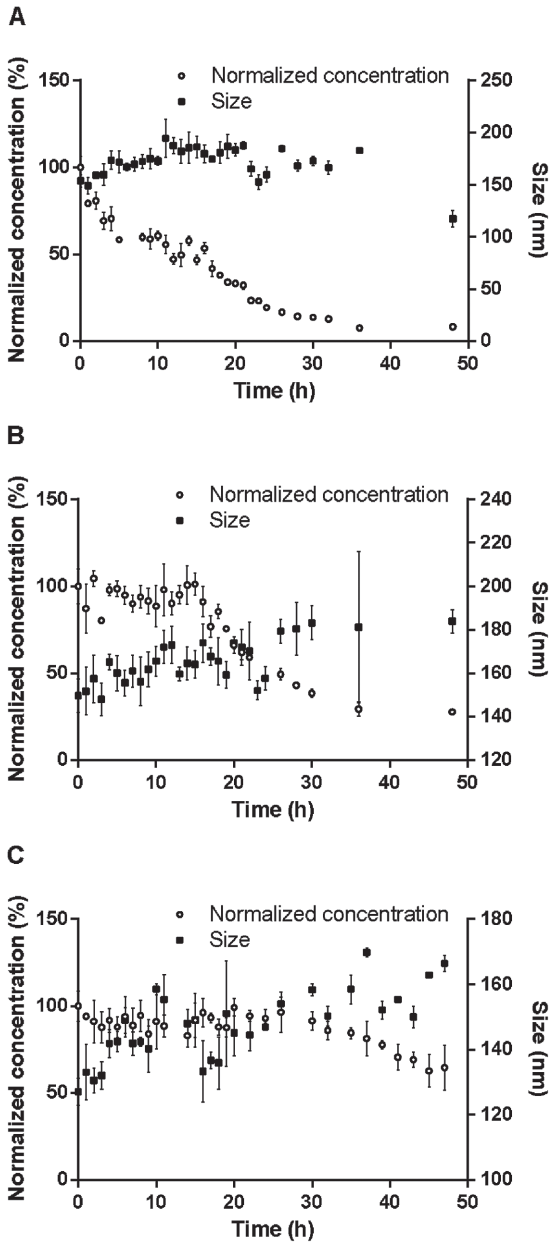

Figure 7. Degradation of pHEMAm-Gly-HEMAm nanogels in PBS at 37 °C measured with nanoparticle tracking analysis (n = 3): A) DS 5 nanogels, B) DS 8 nanogels, and C) DS 20 nanogels.

3.6.3. TEM

The nanogels based on DS 5 pHEMAm-Gly-HEMAm were incubated in buffer at pH 7.4 and at regular time points samples were taken for TEM analysis. As shown in Figure 5, the size of DS 5 pHEMAm-Gly-HEMAm nanogels before incubation measured by TEM is 50–100 nm, which is smaller than that obtained by DLS and NTA (>100 nm). For the DLS and NTA, the particles are hydrated, whereas TEM analysis is done on dried sample, which explains the differences in size between TEM and DLS/NTA. After 2 h and 6 h incubation, the size and shape of particles had hardly changed (Figure 5B,C). After 24 h, no particles were detected with TEM which is in agreement with DLS and NTA results. TEM analysis showed (Figure 5D) that nanogels incubated at pH 5 for 24 h remained their size (50 to 100 nm) and morphology (spherical particles with smooth surface), again demonstrating that in line with DLS data (Figure S14, Supporting Information) hydrolysis of the crosslinks in the nanogels is slowed down at this pH.

3.6.4. Characterization of Water-Soluble Degradation Products of Nanogels

The molecular weights and the amount of water-soluble polymers formed during degradation of the nanogels were determined. Figure 8 shows that nanogels prepared from polymers with different DSs displayed similar degradation trends in terms of an increasing amount of formed water-soluble polymers with time. Figure 8 also shows that in line with the results of DLS and NTA, the degradation rates were slower for nanogels with higher crosslink density (i.e., prepared from polymers with higher DS). More than 60% of soluble polymers were formed as degradation products from DS 5 nanogels after the first 4 h incubation (Figure 8A). After 24 h, about 80% of soluble fragments were formed which is in agreement with DLS and NTA data showing that 80%–90% of nanogels have been degraded in the same time frame. For DS 8 nanogels, 30% of soluble polymer fragments were formed from the nanogels during the first 4 h (Figure 8B). According to the NTA results (Figure 7B), these dissolved fragments did not change the concentration of the nanogel suspension. About 70% of soluble fragments were formed during 48 h incubation, which is in line with the observation during DLS and NTA measurements which showed that about 25% of nanogels remains in the buffer at the same time point (Figures 5B and 6B). In the case of DS 20 nanogels, soluble polymer fragments were continuously formed up to 96 h of incubation (Figure 8C).

Figure 8 also shows that the molecular weights of the formed water-soluble polymers decreased over time, indicating that initially high molecular weight, but soluble fragments were formed that continue to degrade into smaller fragments in the buffer of pH 7.4 and at 37 °C. For DS 20 nanogels (Figure 8C), the molecular weights of soluble polymers could not be recorded in the first 24 h because the amount of polymers was too small to get an accurate determination.

Nanogels with a higher crosslink density showed a delayed increase in the quantities of soluble products as well as a slow decrease in the molecular weights of formed soluble fragments. This can be explained by the longer time that is needed to hydrolyze crosslinks in the

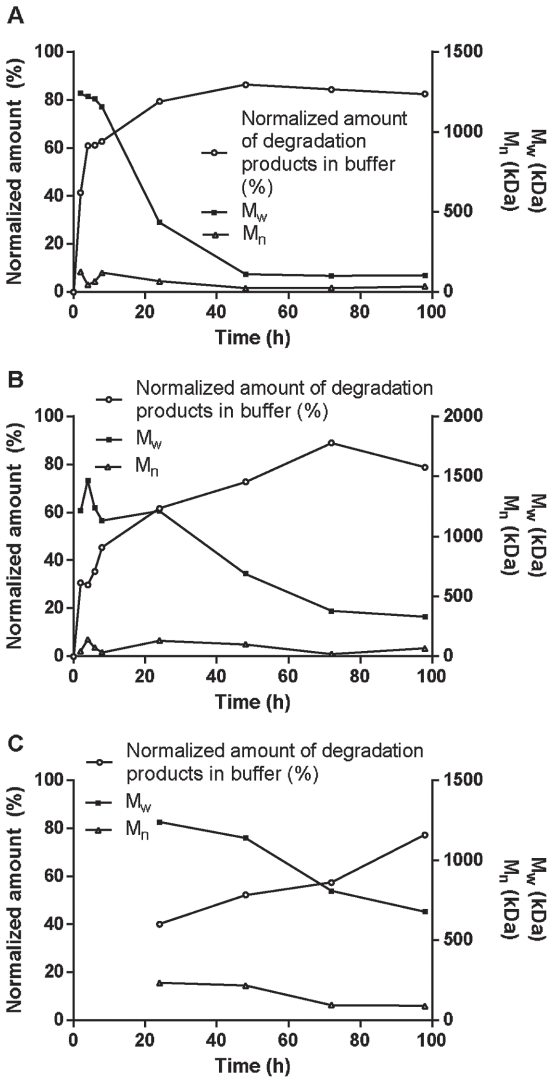

Figure 8. The normalized amount, weight average molecular weight (M_w) and number average molecular weight (M_n) of water-soluble degradation products from pHEMAm-Gly-HEMAm nanogels with different crosslink densities: A) DS 5 nanogels, B) DS 8 nanogels, C) DS 20 nanogels incubated in PBS at 37 °C.

nanogels with a higher crosslink density. After accelerated hydrolysis in 0.02 M NaOH, the side units (i.e., HEMAm-Gly) of polymers (i.e., pHEMAm-Gly-HEMAm) used to prepare nanogels were removed (Figure S4, Supporting Information), and GPC analysis showed that the molecular weights and PDI of the formed water-soluble polymers were the same as the polymer that was used for nanogel preparation (Table 5) which demonstrates that potentially all crosslinks in the nanogels can be hydrolyzed.

Table 5. Characteristics (determined by Viscotek) of pHEMAm used to synthesize the graft copolymers, and water-soluble degradation products of pHEMAm-Gly-HEMAm nanogels after incubation in 0.02 M NaOH for 16 h at 37 °C.

	M_w [kDa]	M_n [kDa]	PDI
Original polyHEMAm	35.1	15.9	2.2
DS 5 nanogels	32.2	14.4	2.2
DS 8 nanogels	32.6	14.2	2.3
DS 20 nanogels	31.9	14.1	2.3

3.7. In Vitro Release of Blue Dextran

Figure 9 shows the release of blue dextran from nanogels with different crosslink densities. Around 80% of the blue dextran loading was released from DS 5 pHEMAm-Gly-HEMAm nanogels during the first 24 h of incubation. On the other hand, DS 8 and DS 20 nanogels showed more sustainable release of blue dextran. For DS 8 nanogels, a complete release of blue dextran was found after 96 h and for DS 20 nanogels, about 70% of blue dextran was released at the end of the experiment.

Blue dextran has a molecular weight of 2 000 000 Da and has a hydrodynamic diameter of 27 nm.[51] This means that given its big size, likely it is initially entrapped in the networks and it can only be released due to degradation of the nanogels. Indeed, Figure 9 shows that the release times very well match those of degradation times of the nanogels (Figure 8) indicating that the release of a macromolecule like blue dextran is governed by degradation of the hydrogel network.

3.8. Cytocompatiblity Studies

In vitro cytocompatibility of the nanogels was investigated using two cell lines: HUVEC cells and RAW 264.7 cells. As human primary cells, HUVECs are commonly used for cytotoxicity tests for biomaterials aimed for i.v. injection. RAW 264.7 cells were also used since macrophages play an important role in innate immunity as well as adaptive immunity. Two assays were used to evaluate the

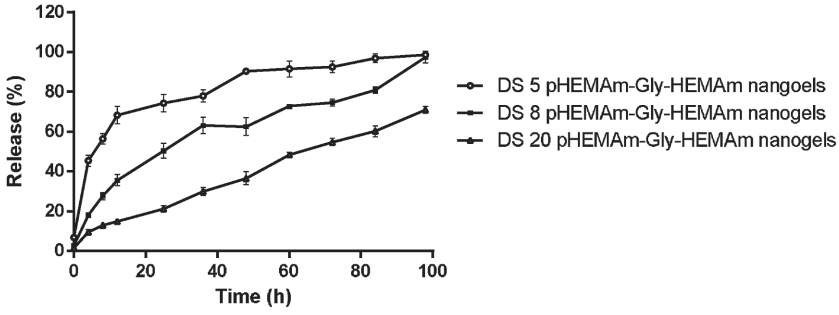

Figure 9. Release of blue dextran from pHEMAm-Gly-HEMAm nanogels in 100×10^{-3} M phosphate buffer (pH 7.4) at 37 °C. ($n = 3$).

cytotoxicity of nanogels. The MTS assay measures the general metabolism as a marker of viable cells;[52] while LDH release can be considered a marker of cell lysis.[53] PLGA nanoparticles were chosen as positive control as they have a proven biocompatibility.[54,55]

The MTS assay (Figure S17, Supporting Information) shows that nanogels with low crosslink density (prepared from DS 4 pHEMAm-Gly-HEMAm) and high crosslink density (prepared from DS 20 pHEMAm-Gly-HEMAm) had no effect on the cell viability on both cell lines in the concentration range tested (up to 2 mg mL^{-1}). The LDH assay (Figure S18, Supporting Information) revealed that LDH leakage even upon incubation of the cells with the highest concentration (2 mg mL^{-1}), the level of LDH leakage was less than 10%. Importantly, pHEMAm-Gly-HEMAm nanogels and PLGA nanoparticles displayed no significant differences using both assays, indicating the cytocompatibility of pHEMAm-Gly-HEMAm nanogels.

4. Conclusions

This paper presents the preparation and characterization of degradable nanogels that can be hydrolyzed in a tailorable manner. These nanogels were produced from pHPAMm-Gly-HEMA and pHEMAm-Gly-HEMAm in which methacrylate groups were coupled to hydrophilic pHPMAm and pHEMAm via biodegradable glycolate esters. Since pHEMAm-Gly-HEMAm hydrolyzed more rapidly than pHPMAm-Gly-HEMA, pHEMAm-Gly-HEMAm nanogels showed faster degradation under physiological conditions. Hydrolysis studies of two types of nanogels with different crosslink densities revealed different degradation times from 24 h to over 4 d under physiological conditions (37 °C and pH 7.4). Our results show that a macromolecule such as blue dextran can be loaded into the nanogels. It was shown that the release of this macromolecule from the nanogels is governed by degradation. These nanogels also showed a good cytocompatibility and they are therefore suitable systems for drug delivery purposes.

Supporting Information

Supporting Information is available from the Wiley Online Library or from the author.

Acknowledgements: This research was partially supported by the China Scholarship Council. The authors would like to thank Lucía Martínez Jothar for providing the PLGA nanoparticles.

Received: January 26, 2016; Revised: February 22, 2016; Published online: April 13, 2016; DOI: 10.1002/mabi.201600031

Keywords: biodegradable; crosslink density; cytocompatibility; drug delivery systems; polymeric nanogels

[1] S. Nayak, L. A. Lyon, *Angew. Chem. Int. Ed.* **2005**, *44*, 7686.
[2] J. K. Oh, R. Drumright, D. J. Siegwart, K. Matyjaszewski, *Prog. Polym. Sci.* **2008**, *33*, 448.
[3] C. Yang, X. Wang, X. Yao, Y. Zhang, W. Wu, X. Jiang, *J. Control. Release* **2015**, *205*, 206.
[4] X. Zhang, S. Malhotra, M. Molina, R. Haag, *Chem. Soc. Rev.* **2015**, *44*, 1948.
[5] J. Zhu, R. E. Marchant, *Expert Rev. Med. Devices* **2011**, *8*, 607.
[6] S. Maya, B. Sarmento, A. Nair, N. S. Rejinold, S. V. Nair, R. Jayakumar, *Curr. Pharm. Des.* **2013**, *19*, 7203.
[7] W. Wu, W. Yao, X. Wang, C. Xie, J. Zhang, X. Jiang, *Biomaterials* **2015**, *39*, 260.
[8] J. Li, B. Jiang, C. Lin, Z. Zhuang, *Int. J. Nanomed.* **2014**, *9*, 5667.
[9] J. Lux, A. G. White, M. Chan, C. J. Anderson, A. Almutairi, *Theranostics* **2015**, *5*, 277.
[10] N. V. Nukolova, H. S. Oberoi, Y. Zhao, V. P. Chekhonin, A. V. Kabanov, T. K. Bronich, *Mol. Pharm.* **2013**, *10*, 3913.
[11] X. Yang, H. Du, J. Liu, G. Zhai, *Biomacromolecules* **2015**, *16*, 423.
[12] P. Pereira, A. Correia, F. M. Gama, *Macromol. Biosci.* **2016**, *16*, 432.
[13] W. Lv, S. Liu, W. Feng, J. Qi, G. Zhang, F. Zhang, X. Fan, *Macromol. Rapid Commun.* **2011**, *32*, 1101.
[14] T. Fernandes Stefanello, A. Szarpak-Jankowska, F. Appaix, B. Louage, L. Hamard, B. G. De Geest, B. van der Sanden, C. V. Nakamura, R. Auzély-Velty, *Acta Biomater.* **2014**, *10*, 4750.
[15] D. Chen, H. Yu, K. Sun, W. Liu, H. Wang, *Drug Deliv.* **2014**, *21*, 258.
[16] A. Concheiro, C. Alvarez-Lorenzo, *Adv. Drug Deliv. Rev.* **2013**, *65*, 1188.
[17] S. S. Pedrosa, C. Gonçalves, L. David, M. Gama, *Macromol. Biosci.* **2014**, *14*, 1556.
[18] B. S. Tucker, S. G. Getchell, M. R. Hill, B. S. Sumerlin, *Polym. Chem.* **2015**, *6*, 4258.
[19] K. Raemdonck, J. Demeester, S. De Smedt, *Soft Matter* **2009**, *5*, 707.
[20] A. V. Kabanov, S. V. Vinogradov, *Angew. Chem. Int. Ed.* **2009**, *48*, 5418.
[21] S. Singh, I. Zilkowski, A. Ewald, T. Maurell-Lopez, K. Albrecht, M. Möller, J. Groll, *Macromol. Biosci.* **2013**, *13*, 470.
[22] K. Ulbrich, V. Šubr, L. W. Seymour, R. Duncan, *J. Control. Release* **1993**, *24*, 181.
[23] K. Ulbrich, V. Subr, P. Podpěrová, M. Burešová, *J. Control. Release* **1995**, *34*, 155.
[24] W. N. E. van Dijk-Wolthuis, J. A. M. Hoogeboom, M. J. van Steenbergen, S. K. Y. Tsang, W. E. Hennink, *Macromolecules* **1997**, *30*, 4639.
[25] J. A. Cadée, M. J. A. van Luyn, L. A. Brouwer, J. A. Plantinga, P. B. van Wachem, C. J. de Groot, W. den Otter, W. E. Hennink, *J. Biomed. Mater. Res.* **2000**, *50*, 397.
[26] J. A. Cadée, M. De Kerf, C. J. De Groot, W. Den Otter, W. E. Hennink, *Polymer* **1999**, *40*, 6877.
[27] J. Kopeček, P. Kopečková, *Adv. Drug Deliv. Rev.* **2010**, *62*, 122.
[28] B. Říhová, M. Kovář, *Adv. Drug Deliv. Rev.* **2010**, *62*, 184.
[29] J. Kopeček, *Adv. Drug Deliv. Rev.* **2013**, *65*, 49.
[30] C. J. Rijcken, C. J. Snel, R. M. Schiffelers, C. F. van Nostrum, W. E. Hennink, *Biomaterials* **2007**, *28*, 5581.
[31] T. Lammers, S. Aime, W. E. Hennink, G. Storm, F. Kiessling, *Acc. Chem. Res.* **2011**, *44*, 1029.

[32] A. S. Sawhney, C. P. Pathak, J. A. Hubbell, *Macromolecules* **1993**, *26*, 581.
[33] N. E. Fedorovich, I. Swennen, J. Girones, L. Moroni, C. A. Van Blitterswijk, E. Schacht, J. Alblas, W. J. A. Dhert, *Biomacromolecules* **2009**, *10*, 1689.
[34] K. Ulbrich, V. Šubr, J. Strohalm, D. Plocová, M. Jelínková, B. Říhová, *J. Control. Release* **2000**, *64*, 63.
[35] D. Neradovic, M. J. van Steenbergen, L. Vansteelant, Y. J. Meijer, C. F. van Nostrum, W. E. Hennink, *Macromolecules* **2003**, *36*, 7491.
[36] C. J. F. Rijcken, T. F. J. Veldhuis, A. Ramzi, J. D. Meeldijk, C. F. van Nostrum, W. E. Hennink, *Biomacromolecules* **2005**, *6*, 2343.
[37] N. Samadi, A. Abbadessa, A. Di Stefano, C. F. van Nostrum, T. Vermonden, S. Rahimian, E. A. Teunissen, M. J. van Steenbergen, M. Amidi, W. E. Hennink, *J. Control. Release* **2013**, *172*, 436.
[38] D. Neradovic, C. F. van Nostrum, W. E. Hennink, *Macromolecules* **2001**, *34*, 7589.
[39] W. N. E. van Dijk-Wolthuis, S. K. Y. Tsang, J. J. Kettenes-van den Bosch, W. E. Hennink, *Polymer* **1997**, *38*, 6235.
[40] R. J. H. Stenekes, W. E. Hennink, *Polymer* **2000**, *41*, 5563.
[41] J. Kopeček, P. Kopečková, T. Minko, Z.-R. Lu, *Eur. J. Pharm. Biopharm.* **2000**, *50*, 61.
[42] L. W. Seymour, R. Duncan, J. Strohalm, J. Kopeček, *J. Biomed. Mater. Res.* **1987**, *21*, 1341.
[43] T. Etrych, V. Šubr, J. Strohalm, M. Šírová, B. Říhová, K. Ulbrich, *J. Control. Release* **2012**, *164*, 346.
[44] S. J. de Jong, E. R. Arias, D. T. S. Rijkers, C. F. van Nostrum, J. J. Kettenes-van den Bosch, W. E. Hennink, *Polymer* **2001**, *42*, 2795.
[45] W. N. E. van Dijk-Wolthuis, M. J. van Steenbergen, W. J. M. Underberg, W. E. Hennink, *J. Pharm. Sci.* **1997**, *86*, 413.
[46] K. Raemdonck, B. Naeye, K. Buyens, R. E. Vandenbroucke, A. Hogset, J. Demeester, S. C. De Smedt, *Adv. Funct. Mater.* **2009**, *19*, 1406.
[47] L. Xu, K. Crawford, C. B. Gorman, *Macromolecules* **2011**, *44*, 4777.
[48] S. Hurrell, R. E. Cameron, *Polym. Int.* **2003**, *52*, 358.
[49] V. V. Vysotskii, O. Y. Uryupina, A. V. Gusel'nikova, V. I. Roldugin, *Colloid J.* **2009**, *71*, 739.
[50] V. Filipe, A. Hawe, W. Jiskoot, *Pharm. Res.* **2010**, *27*, 796.
[51] J. K. Armstrong, R. B. Wenby, H. J. Meiselman, T. C. Fisher, *Biophys. J.* **2004**, *87*, 4259.
[52] A. H. Cory, T. C. Owen, J. A. Barltrop, J. G. Cory, *Cancer Commun.* **1991**, *3*, 207.
[53] H. Vihola, A. Laukkanen, L. Valtola, H. Tenhu, J. Hirvonen, *Biomaterials* **2005**, *26*, 3055.
[54] S. Acharya, S. K. Sahoo, *Adv. Drug Deliv. Rev.* **2011**, *63*, 170.
[55] J. M. Anderson, M. S. Shive, *Adv. Drug Deliv. Rev.* **1997**, *28*, 5.